

AD-771 150

ADVANCED INTERDISCIPLINARY RESEARCH IN
THE DEFENSE APPLICATIONS OF LABORATORY
ASTROPHYSICS

A. V. Phelps, et al

Joint Institute for Laboratory Astrophysics

Prepared for:

Advanced Research Projects Agency
Army Research Office-Durham

August 1973

DISTRIBUTED BY:

NTIS

National Technical Information Service
U. S. DEPARTMENT OF COMMERCE
5285 Port Royal Road, Springfield Va. 22151

ARO 10827.8-P

JOINT INSTITUTE FOR LABORATORY ASTROPHYSICS



UNIVERSITY OF COLORADO

REPORT



NATIONAL BUREAU OF STANDARDS

FINAL REPORT

CONTRACTS NO. DA-31-124-ARO-D-139

AND DAHCO4-72-6-0047

Research Sponsored by

Advanced Research Projects Agency

ARPA Order No. 492

For further information contact:

Dr. A. V. Phelps

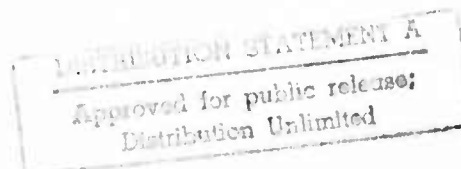
(303)499-1000, X 3604

Dr. S. J. Smith

(303)499-1000, X 3631

University of Colorado
Boulder, Colorado

August 1973



Reproduced by
NATIONAL TECHNICAL
INFORMATION SERVICE
U.S. Department of Commerce
Springfield, MA 01115

AD 771150

29

I. MODELING OF IONIZED GAS SYSTEMS

Program Leader - Dr. A. V. Phelps

Our studies of the modeling of ionized gas systems include a) the theoretical prediction of the conditions for the growth of a constriction in a weakly ionized gas, such as found in a molecular gas laser; b) the development of theories of radiation transport and hydrodynamics applicable to a wider variety of real situations, such as expanding and turbulent plasmas in geometries other than the usual planar geometry; c) the testing of radiative transport theories under controlled laboratory conditions; and d) the experimental determination of the laws of radiative scattering and absorption appropriate to radiative transport problems. The overall objective of this program is to supply experimentally tested understanding and computational techniques required for the analysis and prediction of the role of a) the generation and transport of radiation in plasmas and b) the transport and reactions of charged particles in weak to fully ionized gases. Because of its concern with a number of simultaneous atomic processes and with relatively large numbers of interacting atoms or molecules, this program also provides an important link between the experimental and theoretical determinations of cross sections and rate coefficients which make up much of the remainder of the program and the technology of ionized and excited gases which this work is designed to support.

Stability of Discharges in Weakly Ionized Gases (Drs. E. F. Jaeger,
L. Oster, and A. V. Phelps)

In this theoretical study, numerical calculations have been made of the transient behavior of an infinitely long, cylindrical discharge in helium at pressures from 100 to 1000 Torr. Such calculations are of interest in understanding the stability of weakly ionized gas discharges such as occur in high power molecular lasers.

In contrast with previous calculations¹, full account is taken of the specific heat of the neutral gas, electronic recombination, and the variation of gas pressure in both space and time. Starting with the number, momentum, and energy balances for electrons, ions, and neutrals, we reduce the problem to a set of five time dependent partial differential equations. These include the equation of thermal energy, the ambipolar diffusion equation, the continuity equation for neutrals, and the flux equations for charged and neutral particles. We assume that the discharge is operated in an external circuit with a constant voltage source and impedance. In the numerical solution, the axial electric field in the discharge is recomputed after each time step to account for the decreasing voltage. The ionization and recombination rates along with the transport coefficients for helium have been taken as functions of the axial electric field divided by the gas density from the best experimental measurements currently available.

¹G. Ecker, W. Kröll, K. H. Spatschek, and O. Zöller, Physics Fluids 10, 1037 (1967).

Figs. 1 and 2 illustrate the numerical solution for helium initially at 100 Torr pressure and 300°K with an initial axial electric field of 400 V/cm. The external resistance is 100 ohms per cm length of discharge. The solution is started by turning on the electric field at time zero in the presence of an initial charge density distribution which is a Bessel function falling from 10^{10} cm^{-3} on axis to zero at the wall. The solid lines in Fig. 1 show the transient behavior of the charge density, n , the neutral density, n_n , and the neutral temperature, T_n , computed at the center of the discharge for both 10 and 50 grid points. We find that a spatially uniform pressure approximation (dashed lines in Fig. 1) gives results not far different from the complete solution. In Fig. 2, we compare the constriction of the normalized charge density profile for 50 grid points (dashed curves), and for 10 grid points (solid curves). It is clear from the figure that the spatial resolution afforded by 50 grid points is adequate to produce accurate solutions for the constricted discharge at 100 Torr, while the accuracy of the 10 point solution is better than expected. The constriction of the discharge in our model results from heating of the neutral gas and the consequent outward flow of neutrals. This results in a greater ionization rate at the center of the discharge than at the wall due to the exponential dependence of ionization on the ratio of electric field to gas density. As the charge density increases, the discharge current also increases and the axial electric field must decrease if a constant voltage supply is to be maintained. The instability in Fig. 1 is thus limited by the stabilizing effect of the external circuit, and a steady state is reached. The final approach to steady state is often accompanied by a slight expansion of the charge density profile. The constriction is sometimes preceded by a semistable

plateau in the charge density as occurs in Fig. 1 at about 40 μ secs. This represents an initial, approximate balance between ionization and recombination before there has been significant heating of the gas.

Results computed using the spatially uniform pressure model show the stabilizing effect of higher circuit impedance and the destabilizing effect of lower applied voltage. We also find that either higher recombination coefficients or higher pressures tend to accentuate the constriction. For pressures of 1000 Torr, the constriction proceeds to such an extent that the spatial resolution given by 50 grid points seems no longer adequate.

During the next reporting period these techniques will be extended to an analysis of molecular gases in which attachment is important, e.g., the mixtures used in high power CO_2 lasers.

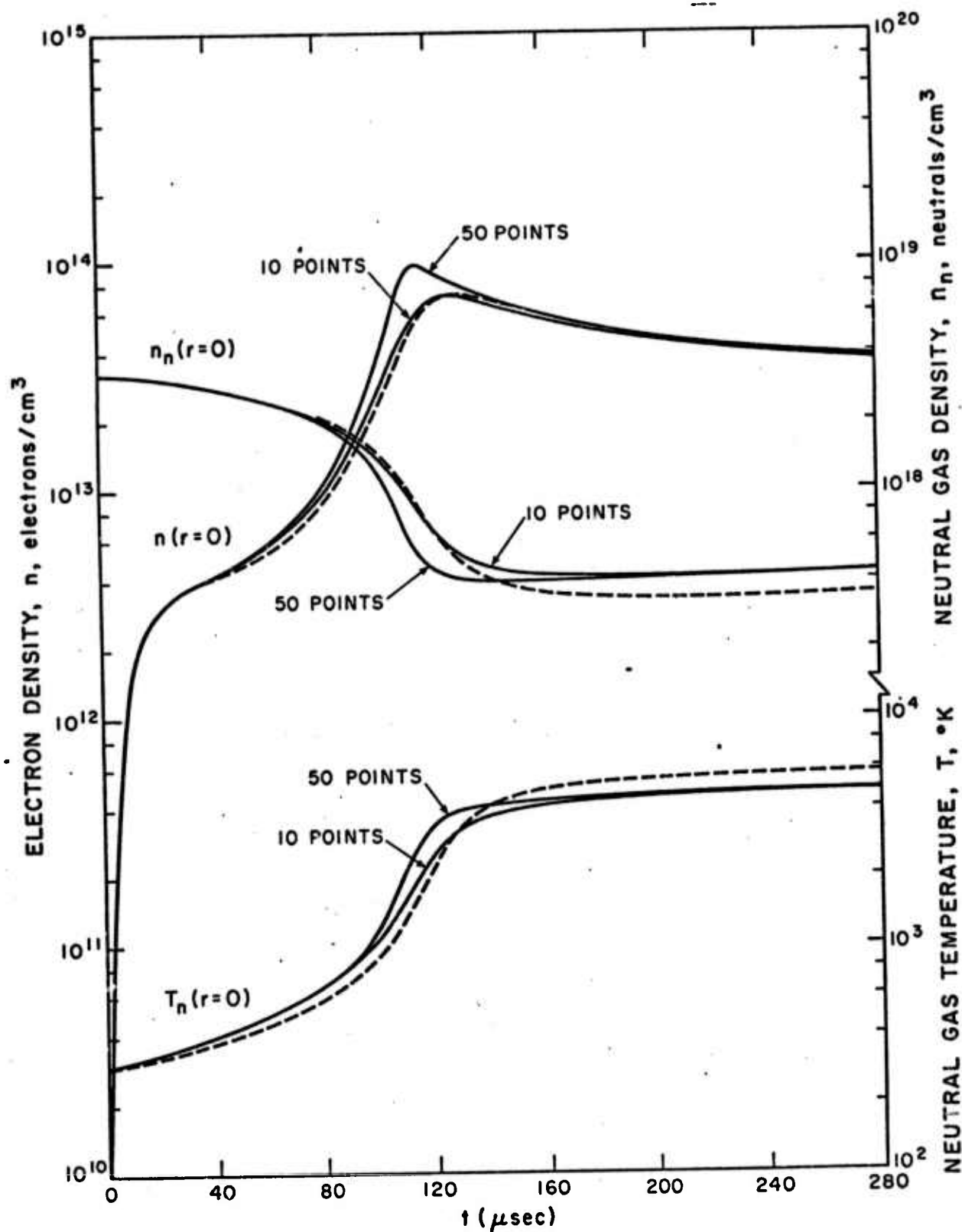


Figure 1. Axial values of charge density, gas temperature, and gas density for helium at 100 Torr pressure. Solid curves are solutions of the complete problem for 10 and 50 grid points. Dashed curves indicate solutions with spatially uniform pressure and 10 grid points.

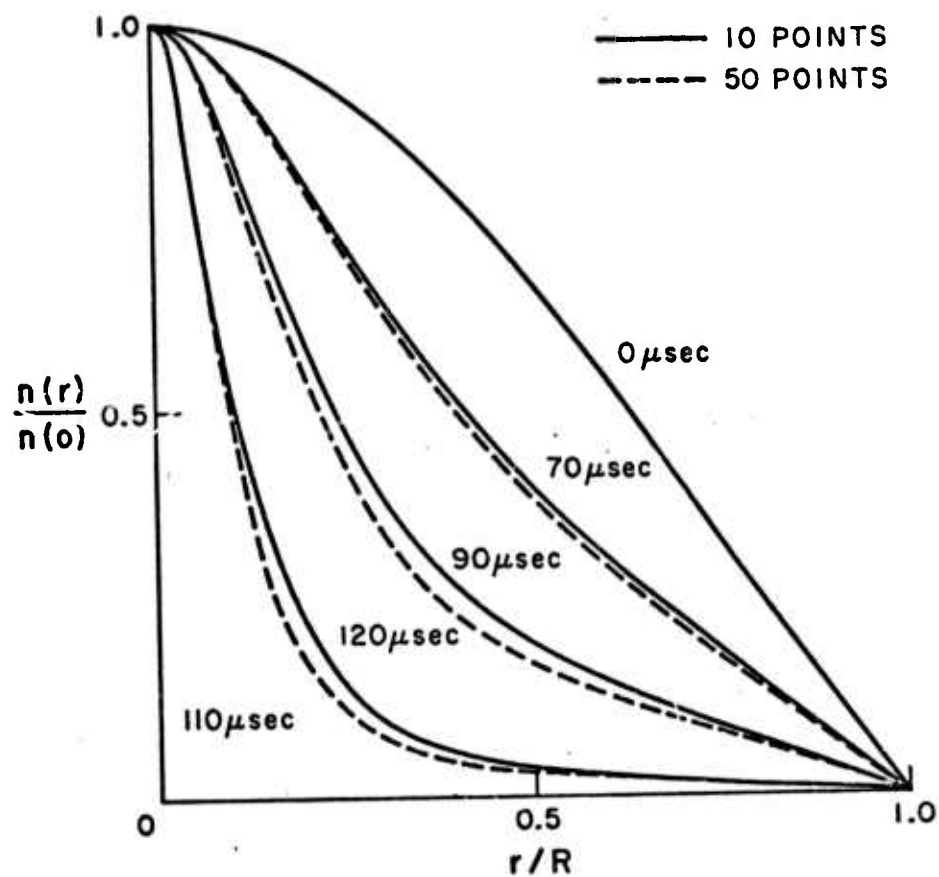


Figure 2. Spatial variation of the charge density normalized to its value on axis for the discharge of Fig. 1. Solid and dashed curves represent the solution for 10 and 50 grid points, respectively.

Scattering and Transport of Resonance Radiation in Gases (Drs. A. V. Phelps and R. Smick)

The objectives of this project are to experimentally determine a) the magnitude and frequency distribution of radiation absorbed and reemitted by an atom for incident frequencies in the vicinity of a collision broadened resonance line, b) the contribution of various scattering and excitation transfer processes to the transport of the energy of atoms excited to a resonance state, and c) the range of validity of various theories of radiative and non-radiative transport of resonance excitation. This project was initiated in order to improve the experimental data and analytical techniques essential to the prediction of a) the rate of radiative energy generation and loss by plasmas containing metal vapor and other atomic line emitters, b) the intensity and frequency distribution of scattered light, e.g., sunlight scattered by sodium, atomic hydrogen, etc., and c) the electrical behavior of nonequilibrium discharge devices in which the resonance atom density is important in determining rates of excitation and ionization, e.g., metal vapor lasers.

An experiment has been assembled to measure the wavelength distribution of light emitted by sodium vapor which has been illuminated with narrowband light from a c. w. laser. Sodium vapor has its lowest-lying excited states connected to the ground state by optically allowed transitions within the tuning range of c. w. dye lasers (the familiar yellow D lines), and we have chosen it as the working substance in spite of its tendency to degrade most optical surfaces.

A sapphire-windowed stainless steel cell with 1 mm. window separation contains the sodium vapor. In order to accurately determine the vapor pressure, we use small metal jacketed thermocouples and an constant-

temperature reference. This also houses stable preamplifiers for the monitoring and for feedback temperature stabilization of the sodium cell.

The input laser power is normalized for changes in both the pulse counting and D.C. outputs of the photomultiplier. The dye laser will produce output radiation narrower than .01 nm, with output power (averaged over 10 sec. intervals) stable to $\pm 10\%$. The system is presently being calibrated.

Radiation Hydrodynamics (Dr. D. G. Hummer and Mr. P. Kunasz)

Line formations in expanding spherical geometries. The method discussed in the last semi-annual report for solving the line formation problem in spherical gaseous configurations with an arbitrary radial velocity field has now been completely coded, checked and used to solve a variety of model problems. The results obtained by running this code with zero velocity are in agreement with the results of the variable Eddington factor code reported in the last semi-annual report. An account of this work has been submitted for publication in the Monthly Notices of the Royal Astronomical Society.

The general conclusion is that velocities up to a few times the mean thermal velocity have a much smaller effect on the source function (proportional to ratio of populations of the upper to the lower state) than does the spherical geometry. On the other hand, even very small velocities (1/10 of the mean thermal velocity) cause significant changes in the radiation field. In particular, the spectral profile of the radiation emerging from the system is distorted in such a way that the long-wavelength side of the line becomes more intense, while the short-wavelength side is reduced in intensity. As in static spherical models, the angular dependence of the emergent radiation is very much more drastic than for plane-parallel situations.

As an example, we consider an isothermal spherical shell with outer radius $R = 30$ times the inner radius R_c . The line opacity is assumed to fall off as r^{-2} and the mean optical thickness of the shell is taken to be $T = 10^3$. A linear velocity law of the form.

$$v(r) = v(R) \frac{(r-R_c)}{(R-R_c)}$$

is assumed, where $v(R)$ is the velocity at the outer radius. The source

function in this case is shown in Figure 3, in units such that the Planck function at line center is unity, for maximum radial velocities $v(R)$ of 0, 1 and 2 in units of the mean thermal velocity. Results are shown for $\epsilon \equiv A_{21}/(C_{21} + A_{21})$ equals to 10^{-2} and 10^{-4} , that is, these systems are very far from local thermodynamic equilibrium. Here A_{21} and C_{21} are the radiative and collisional deexcitation rate coefficients. For comparison, the source functions for static, plane-parallel models, $R/R_c \rightarrow 1$, having the same values of ϵ and T are represented by broken lines. In Figure 4, the spectral profiles for these cases are shown. Here x is the frequency displacement from line center measured in Doppler units.

From these similar results we can conclude that for velocities up to a few times the mean thermal velocity it is satisfactory for most purposes to ignore the effects of the velocity field in computing the source function, which is by far the most expensive part of the calculation, and to include the velocity field only in computing the radiation field from the source function.

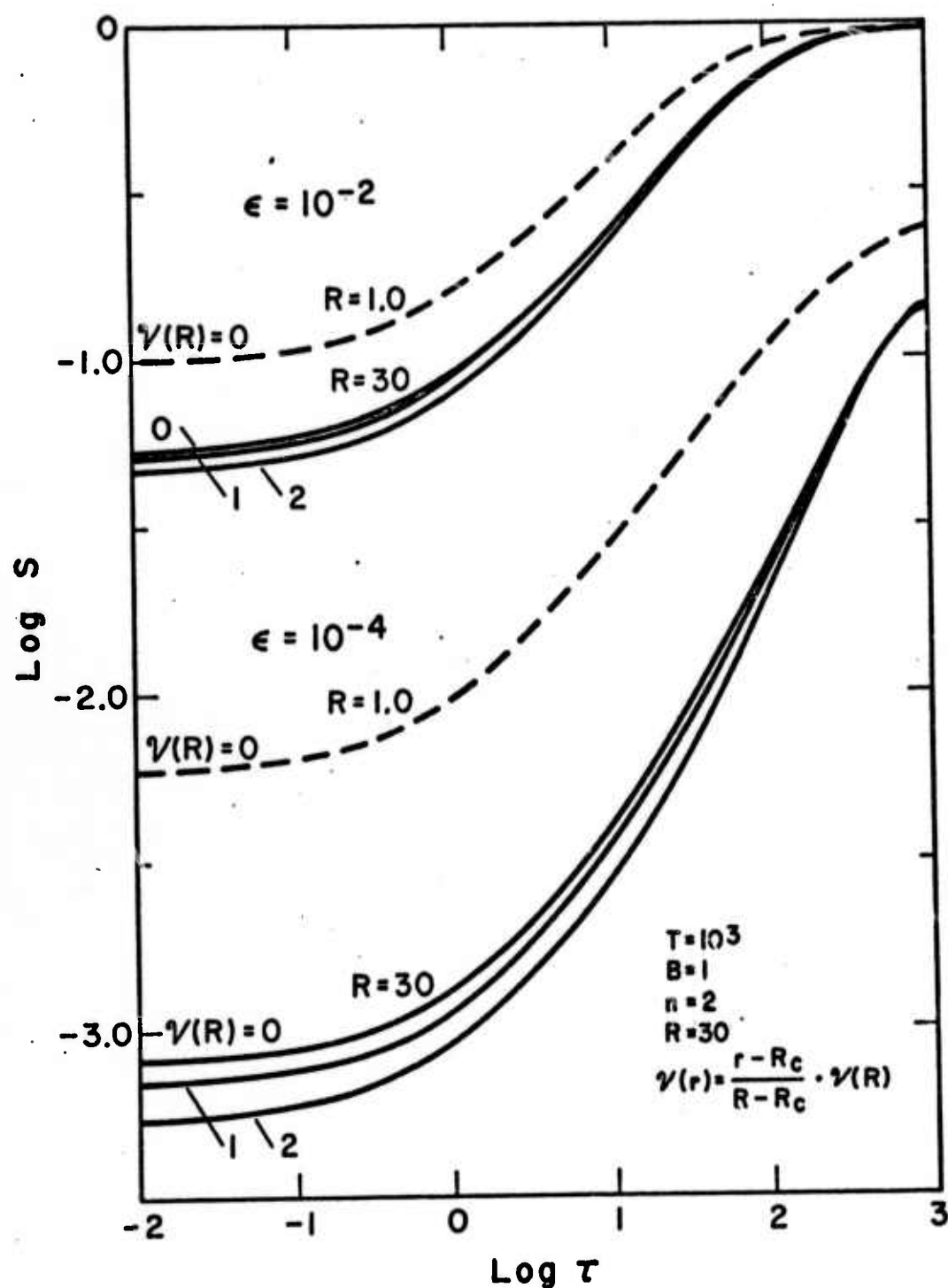


Figure 3. Source functions vs. optical depth from the surface, with curves labeled by value of $v(R)$. Broken lines show corresponding plane-parallel static results.

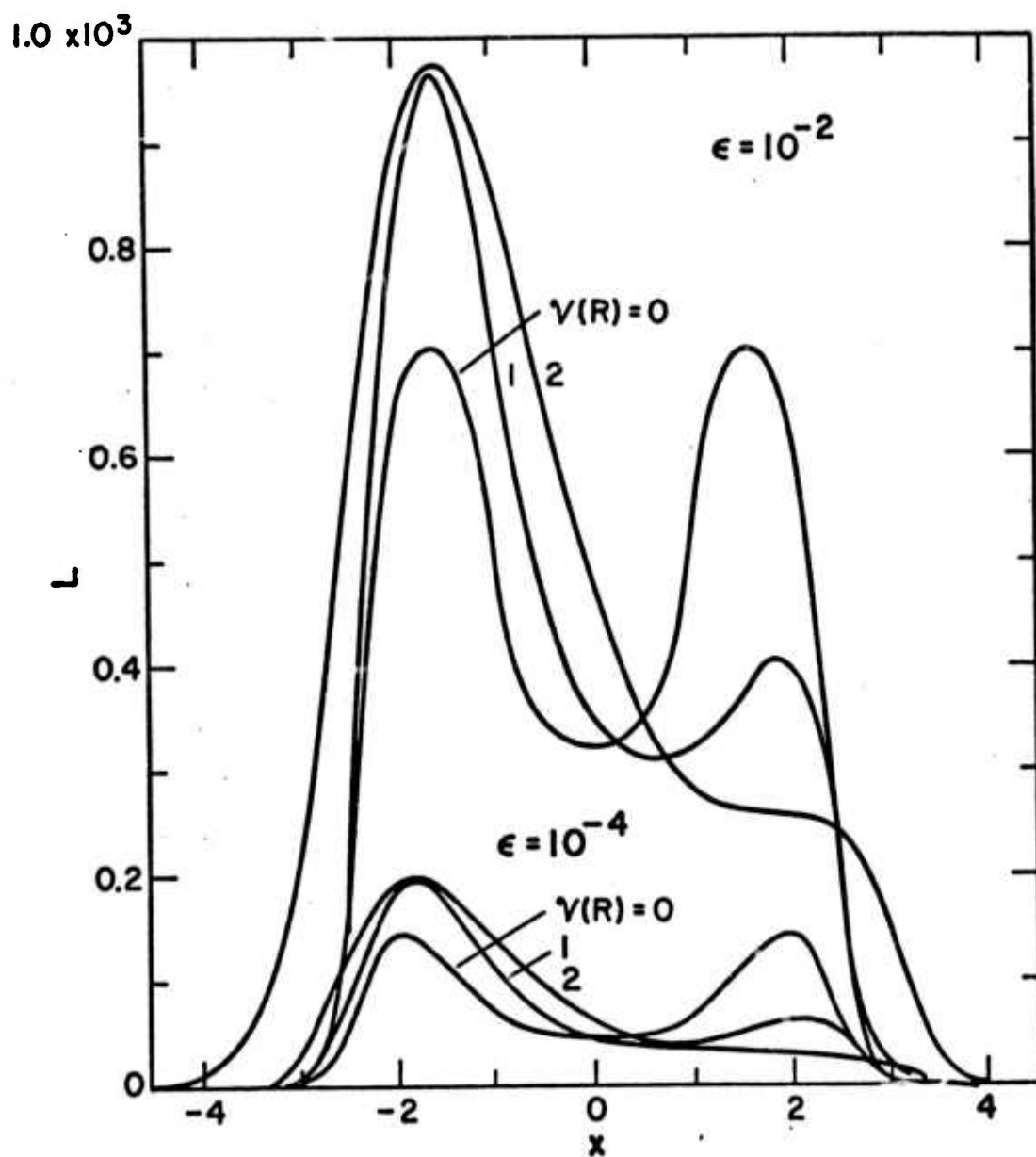


Figure 4. Emergent luminosity (proportional to flux) as a function of frequency displacement $x = (\nu - \nu_0)\Delta_{\text{Doppler}}$.

Plasma Statistics (Dr. W. E. Brittin)

Dr. W. E. Brittin and A. Y. Sakakura have discovered a general quantum mechanical transformation which transforms the usual description in which a system is regarded as being made up of particles (electrons, atomic nuclei) into a description in which the system may be regarded made up of bound composite atoms and "unbound" particles. The composite particle basis looks promising for the treatment of both equilibrium and non-equilibrium processes in many body systems. Both composite and unbound particles enter the theory in a rather simple manner. We expect to continue this work and apply it to systems of interest in practice.

II. TRANSPORT COEFFICIENTS AND REACTION RATES

Program Leader - Dr. S. J. Smith

The prediction of the performance characteristics of ionized gas devices, such as the efficiency, power output and stability of high power lasers, requires that one be able to calculate accurate values of electron transport and reaction rate coefficients for electrons and ions. In order to meet some of these requirements we are engaged in: a) a determination of sets of electron collision cross sections consistent with measured electron transport and ionization coefficients and with recent electron beam measurements of excitation cross sections for the upper excited states of gases found in molecular lasers; b) measurement of cross sections for molecular dissociation; c) evaluation and compilation of low energy electron, photon, and ion collision cross section data; and d) determination of negative ion characteristics, such as single and multiple photodetachment cross sections, negative ion stability and low electron energy scattering parameters.

Electron Transport and Ionization Coefficients (Drs. G. E. Chamberlain,
L. J. Kieffer and A. V. Phelps)

It has been our goal to compile sets of electron collision cross sections consistent with electron transport and rate coefficients in order that these sets of data can be used in the modeling of weakly ionized gas discharges, such as high power molecular gas lasers. To this end we have been working during the past year on creating a critical summary of the measurement techniques for obtaining electron transport and rate coefficients (drift velocity, diffusion, ionization, and excitation).

We are compiling transport data for N_2 in order to:

- (a) compare the data taken by differing techniques,
- (b) look for systematic effects, and
- (c) test our criteria for selection of data and try to estimate the size of systematic errors.

Nitrogen is being used in these studies since we believe most of the problems of measurement, for a non-attaching gas, occur for N_2 ; and a large body of data exists for N_2 .

Currently our summaries of the measurement technique and data collection exist for drift velocity and transverse diffusion (Townsend-Huxley method). Data has been collected for ionization, but work on excitation has not begun. Our recently completed review of transverse diffusion measurements emphasizes the elementary need for varying the geometry, gas density, and electron current to check, for example, for errors due to self space charge, ion space charge, secondaries from ions or photons, and density gradients at the walls. All too often only one point measurements are reported.

Recent reports in the literature have shown that characterization of a swarm by an anisotropic electron diffusion constant improves the interpretation of high precision data and removes the residual dependence

on pressure that existed in some measurements. As a result criteria on the apparatus geometry are available that can be applied to other earlier measurements.

In our current work discussions have been put together of the effect of self space charge on electron swarms, and a discussion of the gas kinetic criteria for a swarm to be in equilibrium. The most universal criteria that can be applied is that the voltage V across the drift space be much larger than the characteristic energy D/μ ,

$$D/\mu \ll V.$$

Equally important is the need to develop a criteria for applicability of the spherical harmonic expansion. This approximation is generally made in calculating velocity distribution functions and relating cross sections to transport coefficients. Hence in calculating distribution functions, and in interpreting experiments in terms of the bulk parameters, drift velocity, diffusion, etc., at high E/N (electric field/gas number density) it is necessary to know the limits of applicability of the spherical harmonic expansion.

Molecular Dissociation Processes (Dr. L. J. Kieffer)

No experimental work was done under this project during this reporting period. Data taken last July have been prepared for publication and are being submitted to Journal of Chemical Physics.

1. "Electron Energy Dependence of the Energy and Angular Distributions of O^- from Dissociative Ion Pair Formation in O_2 " R. J. Van Brunt and L. J. Kieffer.
2. "Breakdown of the Dipole-Born Approximation for Predicting Angular Distributions of Dissociation Fragments" R. J. Van Brunt.

Negative Ion Kinetics (Dr. W. C. Lineberger, Dr. J. Hall, Dr. A. Kasdan, and Mr. T. A. Patterson)

During the present contract period we have completed our studies of the photodetachment of Se^- , OH^- and OD^- . The Se^- results will be published in the Physical Review; the OH^- and OD^- studies will be submitted to the Journal of Chemical Physics. The results of these measurements have been reported in previous Progress Reports.

In recent months both the tunable laser photodetachment spectroscopy device and the fixed laser photoelectron spectroscopy apparatus have been utilized in studies of photodetachment of alkali-negative ions. All of the alkalis have been studied by at least one of the techniques. The resulting electron affinities determined from experiment and from theoretical techniques being developed by Dr. Norcross at JILA are summarized in Table I.

In addition to these direct threshold measurements, there exists the possibility of observing interference effects in photodetachment at photon energies corresponding to the opening of a new channel which competes with an already open channel. This fact was pointed out in detail by Norcross and Moores¹ in the case of Na^- photodetachment at photon energies corresponding to the opening of the lowest ^2P exit channel in the neutral. From a measurement of the photon energy corresponding to the cusp at the channel opening we can determine the electron affinities of the alkalis.

Figure 5 shows Na^- photodetachment data² in the region of the $\text{Na}(3^2\text{P}_{1/2,3/2})$ thresholds. In this case, the wavelength resolution of the tunable laser was not adequate to resolve the individual fine structure thresholds. The cross section shape near threshold corresponds to a Wigner cusp, and is essentially in agreement with calculations performed by

Norcross and Moores.⁵ These data, for various experimental reasons, were quite noisy, and, as a result, there is no reason to believe that the oscillations at long wavelengths are real. From an analysis of these data we find EA(Na) to be $(0.543 \pm .010)$ eV.

The K^- ion is a much more favorable case for experimental study because the expected threshold falls in a spectral region corresponding to a bright laser and the spin-orbit splitting in the excited state is much larger than for Na. Figure 6 shows K^- photodetachment data³ in the vicinity of the $^2P_{1/2,3/2}$ thresholds. In this case, the individual thresholds are well resolved and we find $EA(K) = (0.5012 \pm 0.0005)$ eV. That the observed structure is not a cusp is not bothersome since the general treatment of threshold behavior predicts only a discontinuity in the derivative at the channel opening, but not necessarily a derivative sign change at the threshold.

In some very recent measurements⁴ of Cs^- photodetachment, the threshold behavior is even more unexpected, as seen in Figure 7. The sharp drop in the total Cs^- cross section near 6682 \AA^0 goes, as far as we can tell, to zero. Our present bound on the minimum is 3×10^{-3} of the fully developed cross section, and the shape of the minimum is governed largely by the far wings of the laser line. Note that there also appears to be a discontinuity in the derivative of the total cross section near 6673 \AA^0 . Similar behavior is seen near the $^2P_{3/2}$ threshold, except that the width of the hole is approximately a factor of 2 greater than in the $^2P_{1/2}$ case and the minimum is not nearly so small. We have no a priori way of deciding whether the $P_{1/2}$ channel opening occurs at 6682 \AA^0 or 6673 \AA^0 (corresponding to electron affinities of 0.469 eV and 0.472 eV respectively). Kasdan, however, has used the photoelectron spectroscopy apparatus to measure the

electron affinity of Cs and finds $EA(Cs) = (0.471 \pm 0.003) \text{ eV}$.⁵ His result is suggestive that the higher energy feature is the correct one but not conclusive proof. Norcross⁶ has performed preliminary three-state close coupling calculations on Cs^- photodetachment in the vicinity of the 2P threshold; these preliminary calculations⁶ suggest that there is a doubly excited negative ion configuration which lies very near the 2P threshold. Such a state would give rise to a Fano line shape⁷ with a true zero in the total cross section. The opening of the 2P inelastic channel would interrupt the development of the Fano line shape and give rise to the higher energy cusp observed. If this interpretation is correct, then the higher energy cusp in Cs^- is understood, as is the fact that the $P_{3/2}$ minimum is less dramatic, as well as the qualitative trend of the threshold behaviors through the alkali ion series. As one progresses from sodium to cesium, a temporary negative ion state appears and moves further below the 2P threshold; the development of the resonance line shape corresponding to this state is then interrupted by the opening of the inelastic channel. If this explanation is correct, then we would expect to see a Rb^- behavior which is intermediate between K^- and Cs^- . Such an experiment is now in progress. These temporary negative ion states are frequently seen in electron scattering from neutrals just below excited state thresholds. It may well turn out that cesium represents a typical case, rather than a puzzling exception.

1. D. W. Norcross and D. L. Moores, in Atomic Physics 3, Proceedings of the Third International Conference on Atomic Physics, August, 1972, Boulder, Colorado, edited by S. J. Smith and G. K. Walters (Plenum, N. Y., 1973), pp. 261-67.
2. H. Hotop, T. A. Patterson and W. C. Lineberger, Bull. Am. Phys. Soc. 17, 1128 (1972).
3. H. Hotop, T. A. Patterson and W. C. Lineberger, to be published.
4. T. A. Patterson and W. C. Lineberger, to be published.
5. A. Kasdan, private communication; to be published.
6. D. Norcross, private communications; to be published.
7. U. Fano and J. W. Cooper, Phys. Rev. 137, A1364 (1965); P. G. Burke, in Advances in Atomic and Molecular Physics, edited by D. R. Bates and I. Estermann (Academic, N. Y., 1968), Vol. 4, p. 173; G. J. Schulz, Rev. Mod. Phys., 45, 378 (1973).

TABLE I. ALKALI ELECTRON AFFINITIES (eV)

	Li	Na	K	Rb	Cs
1a	.614	.537	.499	.488	.466
1b	.615	.540	.504	.498	.481
2		.543(10)	.5012(5)	.486(5)p	.472(5)p
3	.617(10)p			.485(10)p	.471(3)p
4	~.61	.53	~.50	.45	~.45

1 Theory - Norcross: a - 2 state calc., b - 3 state calc. (unpublished)
 2 Tunable Laser - Patterson, et al (unpublished)
 3 Photoelectron Spectroscopy - Kasdan, et al (unpublished)
 4 Photodetachment - Feldmann, et al (unpublished)
 p denotes preliminary data

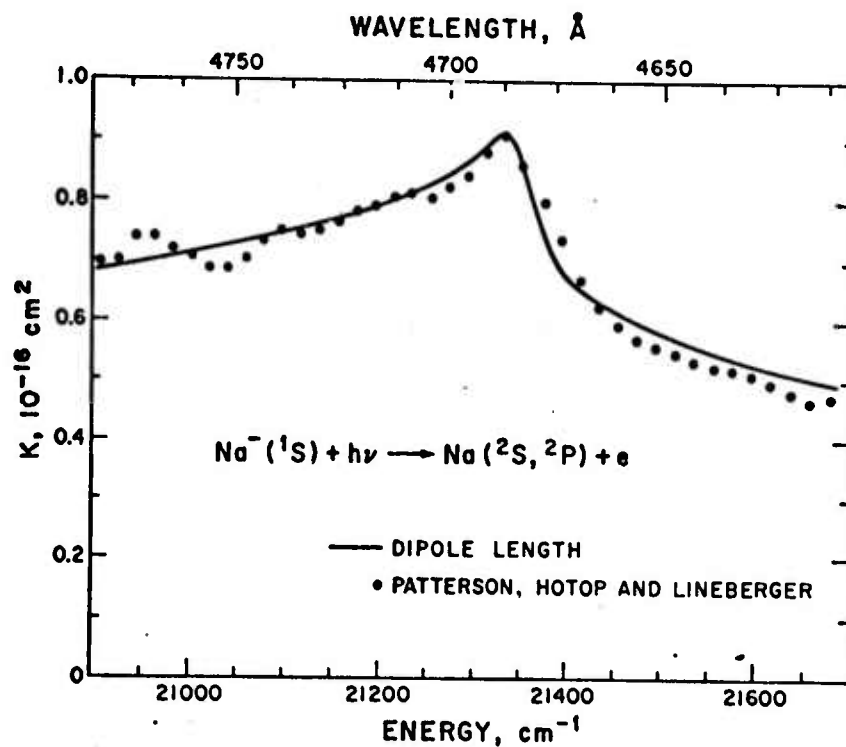


Fig. 5. Na^- photodetachment cross section in the region of the $\text{Na } 3^3\text{P}_{1/2, 3/2}$ thresholds. The cusp occurs at the opening of these ^2P exit channels. The solid line is a close coupling calculation by Norcross and Moores, convolved with our experimental energy resolution.

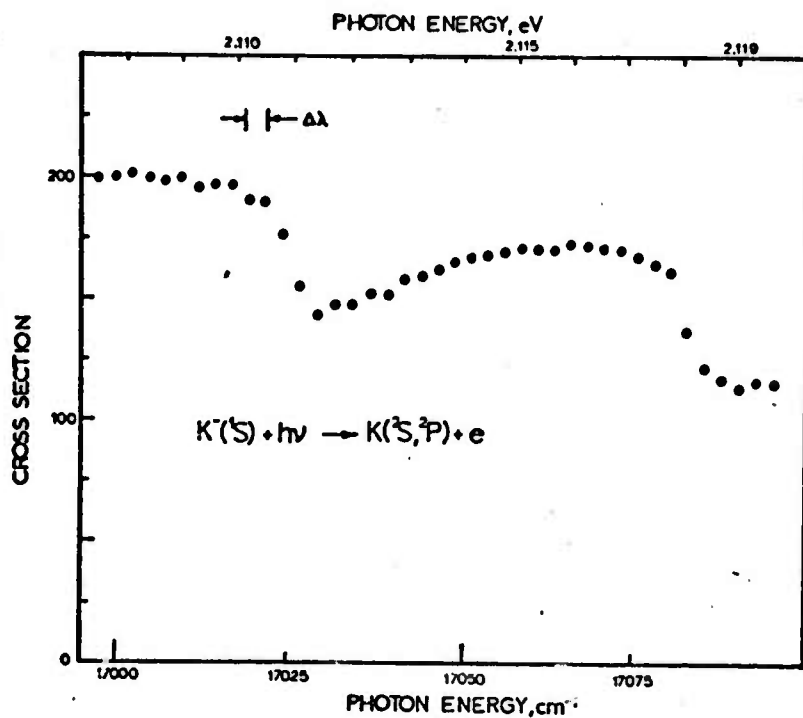


Fig. 6. K^{-} photodetachment data near the 2P thresholds.

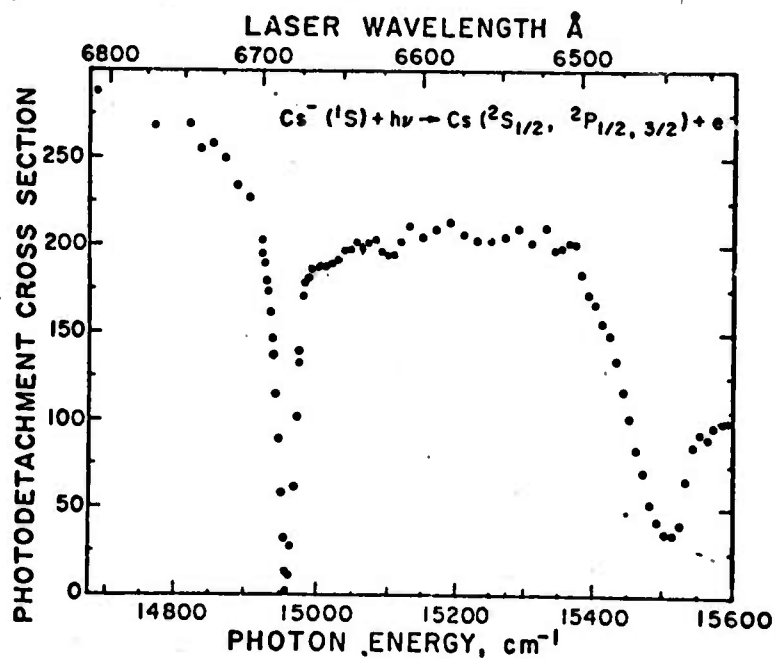


Fig. 7. Cs^{-} photodetachment cross section near the 2P thresholds. The minimum near 6682 Å is broadened by our wavelength resolution. A possible interpretation of this result is discussed in the text.

III. ENERGY LOSS AND RADIATION PRODUCTION BY ELECTRON COLLISIONS

Atomic and Radiation Interaction Theory (Dr. S. Geltman)

Free-free absorption coefficients. This work is now completed and published¹. It includes the calculated free-free absorption coefficients for electrons and the neutral atoms He, C, N, O, Ne, Ar, Kr, and Xe, in the ranges $\lambda = .5$ to $20 \mu\text{m}$ and $T = 500 - 20000^{\circ} \text{K}$.

Angular distributions for ionization. The mathematical problems encountered in applying the Coulomb-projected Born approximation to the ionization of atoms by electron impact have been overcome. Calculations for the triple-differential ionization cross section of hydrogen have been completed, and the method is now being applied to helium.

Interaction of atoms with intense laser fields. A theory has been developed for the absorption of ultraintense radiation by atomic systems. It is now being applied to the bound-free of hydrogen atoms, and will later be applied to the free-free absorption problem. The usual N-photon resonant absorption of the weak radiation perturbation theory is replaced by a non-resonant non-linear absorption in which a monochromatic radiation field produces a continuous distribution of photoionization electrons.

¹S. Geltman, J. Quant. Spectrosc. Radiat. Transfer 13, 601 (1973).

Theoretical Atomic Physics (Drs. D. G. Hummer and D. W. Norcross)

Electron excitation cross sections for atmospheric ions. The elaborate atomic structure models for the Be-like ions C III, N IV and O V were used in preliminary testing runs of the Distorted Wave (DW) collision program for the purpose of establishing convenient data handling procedures. The present application, involving many more reaction channels than in earlier work, would involve the handling of thousands of physical card images if previous procedures were followed. Programs developed to pool, catalogue, sort and retrieve the output of the DW code for use in the program SIMMEG, which completes the calculation of excitation cross sections, were therefore tested and implemented.

Subsequent preliminary runs of the DW program for the larger scattering problems were then undertaken and showed that further alterations in the program were required due to excessive and unnecessary requirements for computer storage. These alterations are now being made, in cooperation with the Department of Physics of the University of London, where the programs were originally developed. Full scale production runs of the programs should begin with the next month.

Electron-Positive Ion Recombination in High Power, CO₂ Lasers (Dr. A. V. Phelps)

As the result of recent experimental evidence by Denes and Lowke¹ that a) the "commercial grade" gases used in high power CO₂ laser contain a fraction of one per cent of H₂O and b) the effective recombination coefficient for typical laser discharge conditions is less than 10⁻⁸ cm³/sec, we have developed a model for the positive ion-molecule reactions and electron-positive ion recombination processes occurring in high power CO₂ lasers using commercial grade gases. This model is consistent with the measurements of electron loss by recombination in N₂ under e-beam laser conditions by Douglas-Hamilton² and the measurements of electron-positive ion recombination for H₃O⁺ by Walls and Dunn, as well as with the discharge conditions of Denes and Lowke. The principal features of this model are:

1) N₂⁺ and CO₂⁺ ions produced by electron impact ionization of N₂ and CO₂ react with H₂O to form H₃O⁺ in times of the order of 0.1 μsec for 0.5% H₂O in typical laser mixture at atmospheric pressure. The N₂⁺ sequence has been observed by Good, Durden and Kebarle⁴. The CO₂⁺ sequence is predicted⁵ to be fast but has not been observed experimentally. The clustered N₄⁺ ion also leads⁴ to H₃O⁺. The H₃O⁺ ions will form clusters with H₂O, with the size of the cluster depending upon the H₂O density, the gas temperature and the mean energy of the ions as they drift through the laser gas mixture.⁶

2) The recombination coefficient measured at JILA by Walls and Dunn³ for monoenergetic electrons and H₃O⁺ decreases as the square of the electron energies for energies above about 0.1 eV. These authors have shown that their electron beam data can be made consistent with the afterglow⁷ and shock tube⁸ experiments and with theoretical threshold laws⁹ by assuming

that the recombination coefficient varies as $(\text{energy})^{-1/2}$ for electron energies below about 0.1 eV. We have made estimates of the effects of departures of the electron energy distribution from a Maxwellian using the distribution functions calculated previously¹⁰ for N_2 and, recently, for various CO_2 laser mixtures¹¹. We also used the approximation that because of the rapid decrease in the recombination coefficient with increasing electron energy, only electrons at the very lowest electron energies are able to recombine with the H_3O^+ , i.e., that the relative recombination coefficients are proportional to the relative number of electrons with energies near zero energy. Figure 8 shows a plot of these relative recombination coefficients as a function of average electron energy for the calculated electron energy distributions in N_2 (solid curve) and for Maxwellian energy distributions (broken curve). Approximate recombination coefficients for electron energies well above 0.1 eV were calculated using the Walls and Dunn data and can be obtained using the right hand scale of Figure 8. Note the more rapid variation with average electron energy of the recombination coefficients calculated using the electron energy distributions for N_2 . A somewhat similar effect is calculated for typical laser mixtures for the higher mean electron energies.

3) The electron-positive ion recombination coefficients measured by Douglas-Hamilton for "commercial grade" N_2 are shown by the points of Figure 8. These data show very nearly the same variation with electron energy as does the solid curve for electrons in N_2 . However, the experimental values are approximately a factor of 3 above the values predicted for H_3O^+ and electrons in N_2 . This comparison suggests the possibility that the positive ions in Douglas-Hamilton's experiment are $\text{H}_3\text{O}^+ \cdot (\text{H}_2\text{O})_n$ and that the electron energy dependence of their recombination coefficients

is similar to that for H_3O^+ . This proposal requires that the magnitudes of the recombination coefficients for the clustered H_3O^+ ions be consistently larger than, for the unclustered ion, as is observed for low energy electrons⁷. It should be noted that as the electric field to gas density ratio E/N and the electron energy are increased the number of water vapor molecules clustered about the H_3O^+ ion will decrease⁶. When this occurs we expect the recombination coefficient to approach that of the solid curve. Measurements of ion breakup in the helium rich laser gas mixtures are not available.

4) If the approximate recombination coefficients given in Figure 8 are extrapolated to the mean energies appropriate to the discharge experiments in N_2 of Denes and Lowke, then one predicts a recombination coefficient for H_3O^+ ions of about $2 \times 10^{-8} \text{ cm}^3/\text{sec}$ compared with a value equal to or less than $10^{-8} \text{ cm}^3/\text{sec}$ obtained from experiment. A slightly smaller value is predicted for H_3O^+ and electrons in typical laser mixtures, e.g., 1:2:3 of $\text{CO}_2:\text{N}_2:\text{He}$, at the discharge E/N .

5) A potentially important effect which we have neglected in Figure 8 is the reduction in the effective recombination coefficient resulting from the depletion of the electron energy distribution function at low energies because of the preferential loss of very low energy electrons by electron- H_3O^+ recombination. From the results of Walls and Dunn and our electron energy relaxation calculations¹⁰ we expect this effect to become significant in N_2 discharges when the fractional ionization exceeds about 2×10^{-5} . This fractional ionization is about an order of magnitude higher than the densities reached in the measurements for N_2 by Denes and Lowke, so that the reduction in the recombination coefficient is probably small. Since the frequency of energy exchange collisions in mixtures containing significant amounts of CO_2 is much larger¹² than for N_2 , an

even larger fractional ionization would be required for most CO_2 laser mixtures in order to reduce the recombination coefficient appreciably. More accurate estimates of this effect will require a more accurate measurement of the low-energy portion of the electron- H_3O^+ or $\text{H}_3\text{O}^+(\text{H}_2\text{O})_n$ recombination coefficient.

6) The significant aspects of the low electron recombination coefficients found by Denes and Lowke and, hopefully, explained by our model are that,

a) one understands the near independence of the operating field strength of the glow discharge phase of laser discharges on discharge current and can make better predictions of the discharge excitation efficiency, impedance characteristics, etc.

b) the unexpectedly low values of the electron-positive ion recombination coefficient for H_3O^+ at electron energies characteristic of discharges suggest the possibility that other ions can be found which will have more desirable recombination coefficients than those found in the pure gases. Thus, a reduction in the electron-positive ion recombination coefficient in a laser in which the ionization is maintained by an external electron beam or by an ultraviolet photon source results in a corresponding reduction in the energy required to maintain the ionization. It is suggested that hydrogen rich ions, as in the NH_3^+ and H_3O^+ studied by Walls and Dunn, are more likely to show unusual energy dependences for the electron-positive ion recombination coefficients because of the relative scarcity of potential energy curve crossings for the neutral and ionized species.

Obviously, all of this model is subject to revision when the crucial mass spectrometric studies of ions are carried out in high pressure, gas laser mixtures and when more data becomes available as to the purity of gases present in laser discharge experiments.

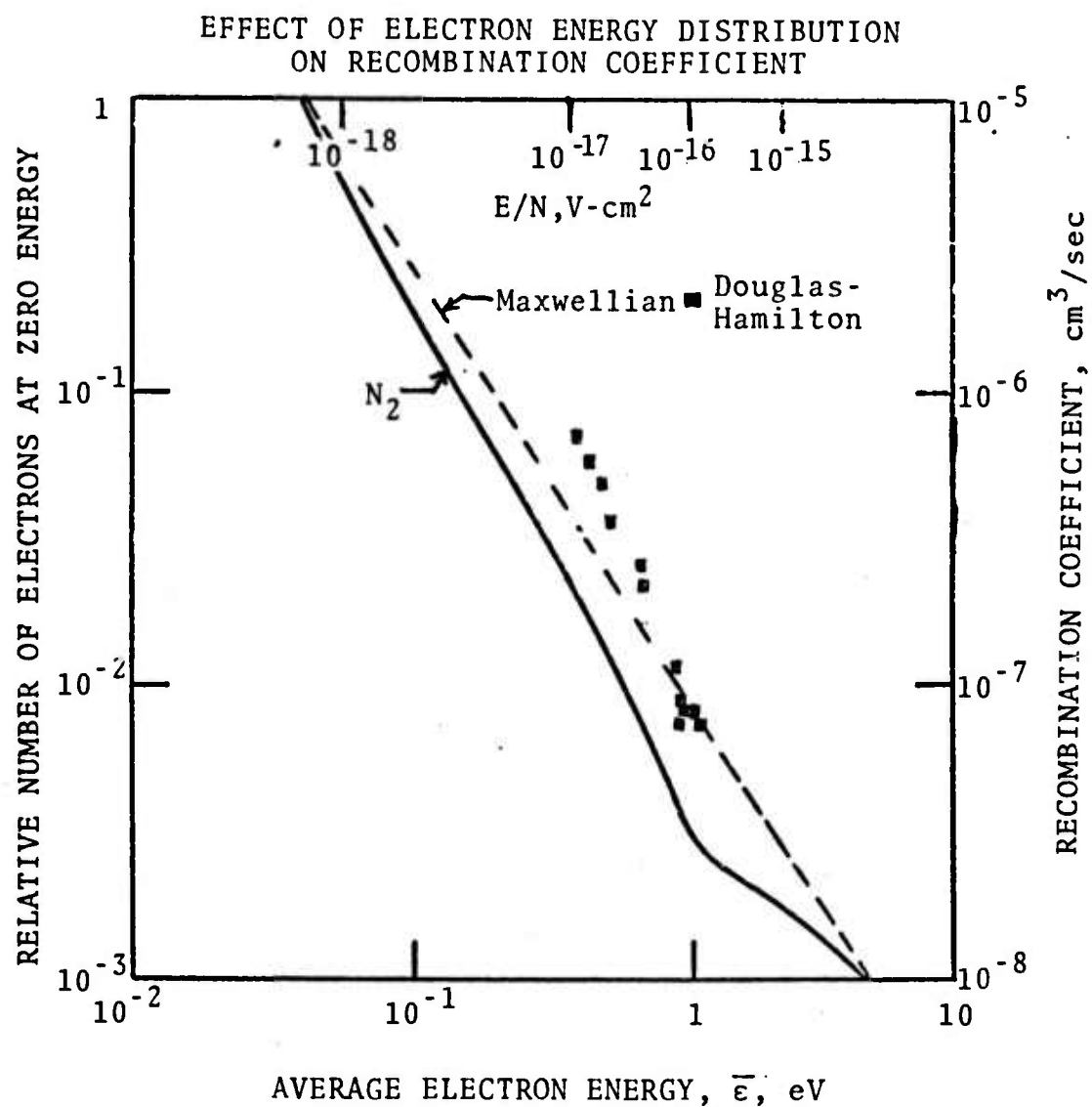


Figure 8. Variation of relative number of electrons at near zero energy and of electron-positive ion recombination coefficient for electrons in N_2 . See text for discussion.

1. L. J. Denes and J. J. Lowke, Appl. Phys. Letters 23, 130 (1973).
2. D. H. Douglas-Hamilton, J. Chem. Phys. 58, 4820 (1973).
3. F. L. Walls and G. H. Dunn (private communication). Work performed under NSF Grant GA-35065. See previous our ARPA Semiannual Reports for a discussion of the technique.
4. A. Good, D. A. Durden and P. Kebarle, J. Chem. Phys. 52, 212 (1970).
5. E. E. Ferguson and F. C. Fehsenfeld (private communication).
6. C. E. Young and W. E. Falconer, J. Chem. Phys. 57, 918 (1972).
7. M. T. Lew, M. A. Biondi and R. Johnsen, Phys. Rev. A 7, 292 (1973).
8. L. N. Wilson and E. W. Evans, J. Chem. Phys. 46, 859 (1967). Note that the positive ions in this experiment are not mass identified and that the measurements are made at an elevated gas temperature as well as electron temperature.
9. J. N. Bardsley and M. A. Biondi, in Advances in Atomic and Molecular Physics, ed. by L. Marton (Academic Press, Inc., New York, 1970).
10. A. G. Engelhardt, A. V. Phelps and C. G. Risk, Phys. Rev. 135, A 1566 (1964).
11. See previous annual reports and J. J. Lowke, A. V. Phelps and B. W. Irwin, J. Appl. Phys. (September) (1973).
12. R. D. Hake and A. V. Phelps, Phys. Rev. 158, 70 (1967).

IV. GENERATION AND ABSORPTION OF RADIATION

Program Leader - Dr. A. C. Gallagher

The objectives of this program are to determine some of the characteristics of alkali metals and alkali metal-rare gas systems of importance in connection with recently proposed tunable lasers¹ utilizing the spectra produced as the result of radiative transitions in molecules having a dissociating ground state. The projects being carried out include the determination of the intermolecular potentials for various alkali metal-rare gas molecules and the cross sections for electron impact excitation of the resonance line of alkali metal atoms.

¹A. V. Phelps, "Tunable Gas Lasers Utilizing Ground State Dissociation," JILA Report 110. September 1972.

Alkali-Inert Gas Line Broadening and Inter-Molecular Potentials (Drs.

A. C. Gallagher and C. G. Carrington)

The objectives of this project are to develop and use techniques for the determination of interaction potentials for excited states of diatomic molecules formed from resonance states and for which the ground state is repulsive or only slightly attractive. Molecular states of this type determine the spectral absorption and emission profiles and the rates of quenching of excited atoms and of depolarization of scattered light when metal vapors are used in a high density of a buffer gas. An exciting application of the radiative properties of such states is the far UV laser reported by Basov and coworkers. Our recent measurements of the spectral distribution of fluorescence in the extreme wings of the cesium and rubidium resonance lines in the presence of inert gas at high densities have been used to obtain the interaction potentials for the ground state and the first two excited states of the cesium- and rubidium-inert gas molecules. The extreme wing fluorescence spectra is analyzed using the quasi-static model of line broadening and readily yields much more detailed information than the previously available measurements of half-width and line shift obtained near the line center. In addition to data yielding interaction potentials, measurements of the variation of the extreme wing intensities at low inert gas densities contain information as to the process of formation of excited molecules in bound states as the result of three-body collisions.

During this reporting period we have developed and tested a new method for learning molecular potentials from continuum spectra. This method is particularly useful for ground-state dissociating molecules such as Xe_2 and LiXe . The molecular potentials and radiative properties of these molecules, which are obtained by this technique, are major determinants

of their behavior in molecular-dissociation laser systems.

The new method for unique determination of the potential compliments the method previously developed under this contract. Whereas the previous method utilized the temperature dependence of high-pressure emission spectra, the new method uses the pressure dependence at one temperature. Thus it is particularly useful for materials such as LiXe, where the temperature-dependence method requires very high temperatures with concomitant problems of containing the highly-reactive lithium. A detailed description of the new method is being prepared for publication.

The obvious advantage of a second potential-determination method is the opportunity to check the self-consistency of potentials obtained by two methods. We have made such a check for the RbXe ground-state dissociating molecule. Each method obtains a set of $A^2\Pi_{1/2}$ and $X^2\Sigma_{1/2}$ potentials; the two sets are compared in Figure 9. The differences between the two sets of potentials are within the combined experimental errors of the two experiments and both sets of potentials yield the same high-pressure RbXe spectrum at 300° K. The reasonable agreement between these two sets of potentials gives us confidence in the models, while the remaining differences point out the need for refinements in the experimental technique.

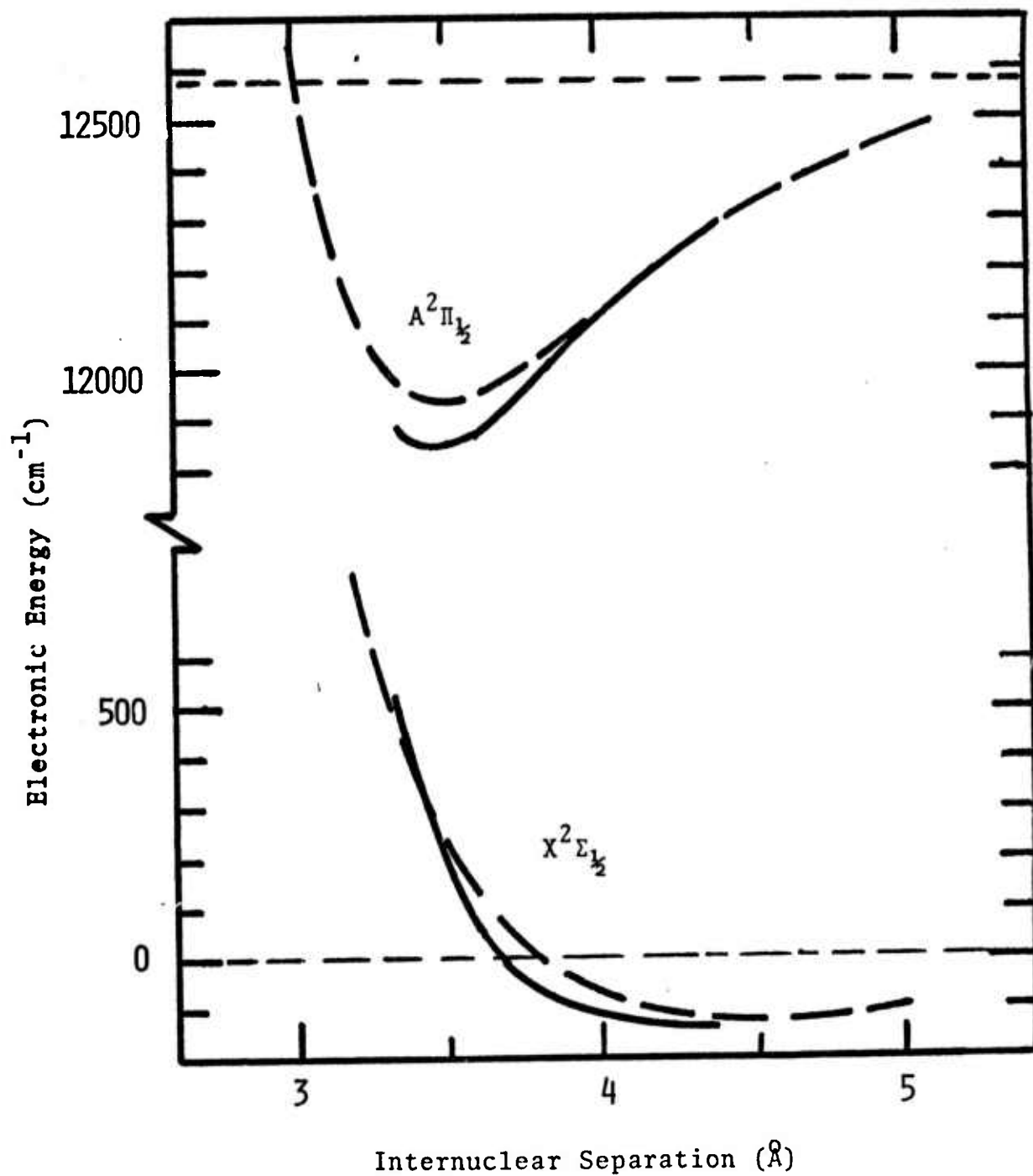


Figure 9. RbXe interaction potentials. The solid lines are obtained from the pressure dependence of the fluorescent intensity. The dashed lines are obtained from the temperature dependence of the fluorescence.

Excitation of Metal Atom Resonance Lines (Dr. A. C. Gallagher and Mr. D. Leep)

Measurements of the cross section for electron excitation of the first excited state of Li have been completed and are being prepared for publication. Figure 10 shows a comparison of these results with one of the theoretical calculations¹. More recent theoretical calculations yield even larger cross sections near the maximum. Experimental data such as this is necessary for the prediction of electron excitation rates in the proposed LiXe laser as well as for testing the close coupling technique being used for the calculation of excitation cross sections for large numbers elements of light mass and high chemical reactivity, e.g., atomic oxygen. These results show the continued importance of experimental measurements of electron scattering from neutral atoms of technological significance.

¹P. G. Burke and A. J. Taylor, J. Phys. B: Atom. Molec. Phys. 2, 869 (1969).

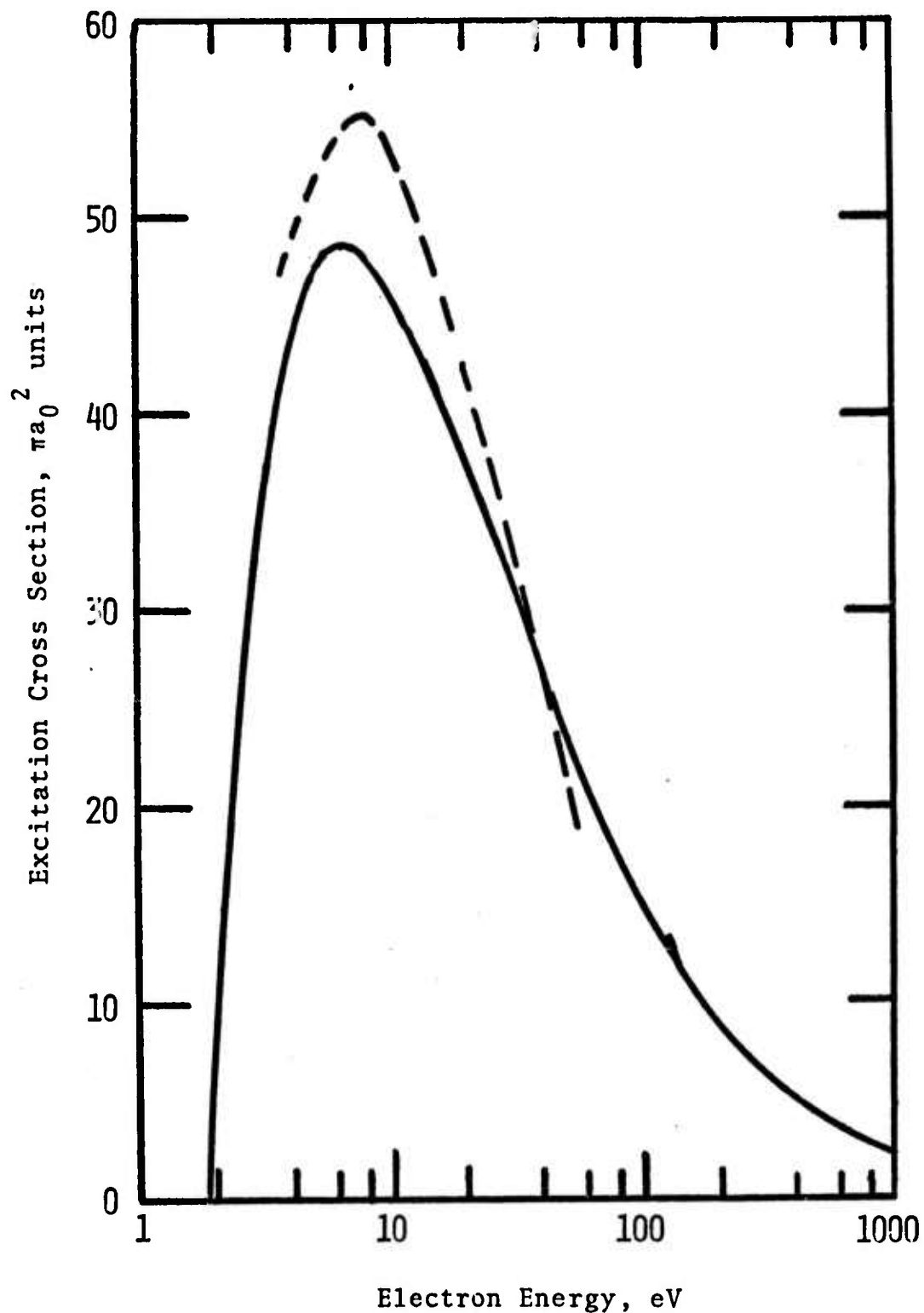


Figure 10. Electron excitation cross sections for excitation of the 2s state of lithium as measured using the 670.7 μ m resonance line (solid curve) and as calculated by Burke and Taylor (dashed curve).

Plasma Spectroscopy (Dr. J. Cooper and Mr. J. Baur)

Work with the pressure driven shock tube (J. Baur) with cesium alum added as a powered aerosol indicates that, at a temperature of 6000° K, electron densities of up to $5 \times 10^{17} \text{ cm}^{-3}$ can be easily obtained. Measurements of electron density have been performed using a two wavelength interferometer (in a Michelson arrangement) and also using the Stark broadening of H- α . Consistency of the measurements are to about 10%. The Stark broadening of both the calcium II H & K lines and the sodium D lines are being measured. At the low temperatures considered here, the Stark broadening is increasing rapidly with decreasing temperature. For calcium II 3968° Å, the ratio of width to electron density at 5000° K is roughly twice that at $20,000^{\circ}$ K, which is consistent with theoretical predictions.

Theoretical work has been performed on several aspects of resonance broadening. It is found that coherent transfer of excitation from one excited atom to another ground state atom leads to a shift of the resonance line itself, but for radiation terminating on the upper level of the resonance transition there are no additional line broadening effects (other than those included in the traditional impact theory). When two identical atoms (a fixed distance apart) interact via their radiation field it is possible to form both a symmetric and an antisymmetric combination of states. At small distances the symmetric (super radiant) state decays with twice the rate associated with an isolated atom, whereas the decay of the antisymmetric state is very small. We have examined the role of relative motion (Doppler effect) on this coherent interaction, and find that the radiative coupling is reduced to essentially zero so that these states decay as for isolated atoms when the atoms can move a distance of roughly $\lambda/2$ in their natural lifetime.

Manuscripts Involving ARPA Funds

Listed below are papers submitted for publication during the period covered by this report.

- S. Geltman, "Free-free radiation in electron-neutral atom collisions," J. Quant. Spectrosc. Radiat. Transfer 13, 601 (1973).
- H. Hotop, R. A. Bennett and W. C. Lineberger, "The electron affinities of Cu and Ag," J. Chem. Phys. 58, 2373 (1973).
- H. Hotop and W. C. Lineberger, "Dye-laser photodetachment studies of Au⁻, Pt⁻, PtN⁻, and Ag⁻," J. Chem. Phys. 58, 2379 (1973).
- H. Hotop, W. C. Lineberger and T. A. Patterson, "Experimental investigation of the photodetachment threshold law," to appear in VIII International Conference on the Physics of Electronic and Atomic Collisions: Abstracts of Papers (in press).
- H. Hotop, T. A. Patterson and W. C. Lineberger, "High resolution photodetachment studies of negative ions," in Advances in Mass Spectroscopy, Vol. VI (in press).
- H. Hotop, T. A. Patterson and W. C. Lineberger, "High resolution photodetachment study of Se⁻ ions," to appear in Phys. Rev. A.
- W. C. Lineberger, "Photodetachment of negative ions," in Theoretical Chemistry, Proceedings of the Summer Research Conference on Theoretical Chemistry, June 1972, Boulder, Colorado (Wiley, New York, in press).
- W. C. Lineberger, "Laser negative ion spectroscopy," in Laser Spectroscopy, Proceedings of the Laser Spectroscopy Conference, June 1973, Vail, Colorado (Plenum, New York, in press).
- T. A. Patterson, H. Hotop and W. C. Lineberger, "Photodetachment of alkali negative ions," to appear in VIII International Conference on the Physics of Electronic and Atomic Collisions: Abstract of Papers (in press).
- A. V. Phelps, "Tunable gas lasers utilizing ground state dissociation," JILA Report No. 110, September 15, 1972.
- B. W. Woodward, V. J. Ehlers and W. C. Lineberger, "A reliable, repetitively pulsed, high-power nitrogen laser," to appear in Rev. Sci. Instr.
- B. W. Woodward, W. C. Lineberger and L. M. Branscomb, "Ionization of cesium atoms in collisions with atomic oxygen," submitted to Phys. Rev. A.